An Interpretive Basis of the Hyperfine Shifts in Cyanide-Inhibited Horseradish Peroxidase Based on the Magnetic Axes and Ligand Tilt. Influence of Substrate Binding and Extensions to Other Peroxidases

Gerd N. La Mar,* Zhigang Chen, K. Vyas, and Andrew D. McPherson

Contribution from the Department of Chemistry, University of California, Davis, California 95616

Received August 8, 1994[⊗]

Abstract: The ^{1}H NMR hyperfine shift pattern for nonheme resonances in low-spin ($S = 1/2$) cyanide-inhibited horseradish peroxidase, HRP-CN, and cytochrome *c* peroxidase, C*c*P-CN, are interpreted in terms of the anisotropy and orientation of the paramagnetic susceptibility tensor in the molecular framework. The orientation of the axes is obtained from a least-squares search for the Euler angles which will rotate the metal-centered crystal coordinates to a coordinate system (the magnetic axes) which quantitatively account for the observed dipolar shifts. Previous 2D NMR has shown that the key active site residues in HRP-CN (Chen, Z.; de Ropp, J. S.; Hernández, G.; La Mar, G. N. *J. Am. Chem. Soc.* **1994**, *116*, 8772) occupy essentially the same position in the active site as in the crystal structure of C*c*P-CN, such that the crystal coordinates for select protons of C*c*P-CN could be used for both HRP-CN and C*c*P-CN NMR analysis. The validity of the magnetic axes description for HRP-CN is supported by the excellent correlation between observed and predicted dipolar shifts, by the ability to predict the shifts for residues not conserved between C*c*P and HRP, by the quantitative prediction of the influence of substrate binding on the hyperfine shifted pattern in HRP-CN, and by accounting for the significant variation in hyperfine shift pattern among cyanide-inhibited heme peroxidases genetic variants which possess very similar molecular structure. The major magnetic axis is found tilted (~20°) from the heme normal in both C*c*P-CN and HRP-CN, and is similar to that of the Fe-CN tilt in the C*c*P-CN crystal structure. The effect of binding the substrate benzhydroxaminic acid to HRP-CN is to decrease the tilt of the Fe-CN unit by 9° away from the BHA binding site. The distinct patterns of hyperfine shifted for the cyanide-inhibited lignin and manganese peroxidases indicate that these proteins exhibit significantly less tilt (~5°) of the Fe-CN unit from the heme normal than C*c*P-CN or HRP-CN.

Introduction

Heme peroxidases comprise a superfamily of enzymes that catalyze the oxidation of organic and inorganic substrates at the expense of hydrogen peroxide.[1,2] They share very similar reactive intermediates that are two (compound **I**) and one (compound **II**) oxidizing equivalents above the ferric resting state. Both activated complexes contain a ferryl ion, with the former also possessing a cation free radical on either the heme or a nearby amino acid side chain. While the sequences for classical peroxidases can vary significantly,[2] they also exhibit strongly conserved segments attributed to the active site. Detailed crystallographic studies, first on cytochrome *c* peroxidase,[3,4] C*c*P,[5] and, more recently, ligning peroxidase,[6] LiP, have shown that certain aspects of the active site structures are highly conserved. The essential catalytic residues have been proposed[4] to consist of a proximal His whose ring is hydrogen bonded to an Asp to stabilize the higher oxidation states of compounds **I** and **II**, and a distal His and Arg to serve, respectively, as general base and to facilitate heterolytic bond cleavage for the ligated peroxide. However, while the available data provide a picture that rationalizes many of the similarities among the various peroxidases, there are still many properties, such as substrate binding sites, redox potential, acid−base properties, etc., which clearly differentiate the peroxidases and that are not nearly as well understood.

For horseradish peroxidase, HRP, the most extensively studied peroxidase, the absence of suitable crystals has placed a strong emphasis on spectroscopic characterization of its structure.[7,8] NMR of low-spin ferric heme peroxidase complexes can provide not only detailed information on the molecular structure in a

* Address correspondence to this author.

[⊗] Abstract published in *Advance ACS Abstracts*, December 1, 1994.

(1) For reviews, see: Dunford, H. B.; Stillman, J. S. *Coord. Chem. Rev.* **1976**, *19*, 187−251. Bosshard, H. R. *Peroxidases in Chemistry and Biology*; Everse, J., Everse, K. E., Grisham, M. B., Eds.; CRC Press: Boca Raton, FL, 1991. Welinder, K. G. In *Plant Peroxidases 1980−1990: Progress and Prospects in Biochemistry and Physilogy*; Gaspar, T., Penel, C., Greppin, H., Eds.; University of Geneva Press: Geneva, Switzerland, 1992; pp 1−24.

(2) Welinder, K. G. *Eur. J. Biochem.* **1979**, *96*, 483−502. Welinder, K. G. *Eur. J. Biochem.* **1985**, *151*, 497−504. Welinder, K. G. *FEBS Lett.* **1976**, *72*, 19−23. Welinder, K. G.; Gajhede, M. In *Plant Peroxidases: Biochemistry and Physiology;* Welinder, K. G., Rasmussen, S. K., Penel, C., Greppin, H., Eds.; University of Geneva Press: Geneva, Switzerland, 1993, pp 35−42.

(3) Edwards, S. L.; Poulos, T. L. *J. Biol. Chem.* **1990**, *265*, 2588−2595.

(4) Poulos, T. L.; Kraut, J. *J. Biol. Chem.* **1980**, *255*, 8199−8205. Finzel, B. C.; Poulos, T. L.; Kraut, J. *J. Biol. Chem.* **1984**, *259*, 13027−13036.

(5) The abbreviations used are: C*c*P, cytochrome *c* peroxidase; HRP, horseradish peroxidase; LiP, lignin peroxidase; metMbCN, cyano metmyoglobin; BHA, benzhydroxaminic acid; NOESY, 2D nuclear Overhauser spectroscopy; TOCSY, total correlation spectroscopy; WEFT, water elimination Fourier transformation; DEFT, driven equilibrium Fourier transformation; DSS, 2,2-dimethyl-2-silapentane-5-sulfonate.

(6) Edwards, S. L.; Raag, R.; Wariishi, H.; Gold, M. H.; Poulos, T. L. *Proc. Natl. Acad. Sci. U.S.A.* **1993**, *90*, 750−754. Poulos, T. L.; Edwards, S. L.; Wariishi, H.; Gold, M. H. *J. Biol. Chem.* **1993**, *268*, 4429−4440.

(7) Dunford, H. B. In *Peroxidases in Chemistry and Biology*, Vol. II; Everse, J., Everse, K. E., Grisham, M. B., Eds.; CRC Press: Boca Raton, FL, 1991; pp 1−23.

(8) (a) de Ropp, J. S.; La Mar, G. N.; Smith, K. M.; Langry, K. C. *J. Am. Chem. Soc.* **1984**, *106*, 4438−4444. (b) Thanabal, V.; de Ropp, J. S.; La Mar, G. N. *J. Am. Chem. Soc.* **1987**, *109*, 265−272. (c) Thanabal, V.; de Ropp, J. S.; La Mar, G. N. *J. Am. Chem. Soc.* **1987**, *109*, 7516−7525. (d) Thanabal, V.; de Ropp, J. S.; La Mar, G. N. *J. Am. Chem. Soc.* **1988**, *110*, 3027−3035.

0002-7863/95/1517-0411$09.00/0

manner similar to that usually pursued by crystallographic methods, but also yields unique information on the electronic structure and magnetic properties of the active site.[8-15] Thus 2D NMR methods have been demonstrated to provide unambiguous assignment of active site residues and quantitative disposition of the residues relative to each other and to the heme for HRP-CN.[9,10] On the other hand, while the molecular structure of cyanide-inhibited heme peroxidases can now be elucidated, there still does not exist an intepretive basis for their remarkably variable hyperfine shifts. The wealth of information contained in these hyperfine shifts is emphasized by their exquisite sensitivity to the genetic origin of the protein,[8-13] site directed mutagenesis for a given protein,[14] and substrate binding.[15]

Inspection of the available ^{1}H NMR data on cyanide complexes of classic heme peroxidases[8-15] reveals that the pattern of the heme resonance, which is dominated by scalar or contact shifts that can be related to the orientation of the axial His imidazole plane relative to the heme,[16,17] is similar. On the other hand, the noncoordinated catalytic residues, which exhibit only dipolar shifts,[17] can exhibit remarkably different shift patterns, in spite of the fact that their stereochemistry in the heme pocket is highly conserved.[3,4,6] The dipolar shift, δ_{dip}, is given by the equation

$$\delta_{dip} = \frac{1}{2N}\left[\Delta\chi_{ax}GF_{ax} + \frac{3}{2}\Delta\chi_{rh}GF_{rh}\right]R(\alpha,\beta,\gamma) \qquad (1)$$

where $\Delta\chi_{ax} = \chi_{zz} - {}^1/_2(\chi_{xx} + \chi_{yy})$ and $\Delta\chi_{rh} = \chi_{xx} - \chi_{yy}$ are the axial and rhombic anisotropies of the paramagnetic susceptibility tensor, χ; $GF_{ax} = (3\cos^2\theta - 1)r^{-3}$ and $GF_{rh} = (\sin^2\theta\cos 2\Omega)r^{-3}$ are the axial and rhombic geometric factors evaluated in an arbitrary metal-centered coordinate system, x', y', z', (Figure 1) usually obtained from X-ray coordinates; $R(\alpha,\beta,\gamma)$ is the Euler rotation that converts the pseudosymmetry coordinate system, x', y', z', into the magnetic coordinate system, x, y, z, for which χ is diagonal. Variation in observed δ_{dip} requires changes in the anisotropy, geometric factors, or orientation of the magnetic axis, possibly all three. For cases where the magnetic anisotropies are invariant, and the molecular structure (GF) is conserved, changes in δ_{dip} must originate from changes in $R(\alpha,\beta,\gamma)$.

Detailed studies of both natural genetic variants and synthetic point mutants of isoelectronic cyano metmyoglobin,[17] metMbCN, have shown that highly variable hyperfine shift patterns for nonheme protons can be quantitatively interpreted in terms of variable orientation of a fixed anisotropic magnetic susceptibility tensor χ. The orientation of the major (or z) axis was found to be related the Fe-CN tilt, while the rhombic axes were aligned with the axial His imidazole plane. Moreover, all changes in the orientation of the major magnetic axis could be correlated with the expected steric influences on the Fe-CN tilt due to distal mutations. It is likely, therefore, that the disparate ^{1}H NMR hyperfine shift patterns for the various plant and fungal cyanide-inhibited peroxidases[8-13] reflect primarily difference in the orientation of the magnetic axes.

Among the heme peroxidases, the necessary high resolution crystal coordinates to determine GF in eq 1 are available only for C*c*P[3,4] and LiP.[6] A crystal structure is in progress on the basic E5 isozyme of HRP,[18] but the resolution is sufficient only to establish a folding pattern homologous to C*c*P, and does not yet provide accurate atomic coordinates. In contrast, the most extensive and definitive set of NMR assignments for the active site are available for HRP-CN.[8-10] However, detailed analysis of the NOE pattern among residues, and between the residues and the heme, as well as iron-induced paramagnetic relaxation, have shown[8-10] that several important structural features of HRP-CN, namely, the orientation of the proximal helix relative to the heme, and the dispositions of the distal Arg and His relative to each other and to the heme, are highly conserved with respect to C*c*P. This suggests the possibility that the crystal coordinates for structurally conserved residues in C*c*P,[3] together with the unambiguous and extensive NMR assignments in HRP-CN,[10] allow the determination of the magnetic axes in the latter complex. The residues for which resonances have been assigned, and their schematic positions in the heme pocket, are shown in Figure 1.

Resonable criteria for validating this approach are: (1) the magnetic axes determined on the basis of the available, but more limited, C*c*P-CN NMR data[11] can be related to the deformation of the Fe-CN unit in the C*c*P-CN crystal structure;[3] (2) similar magnetic axes are obtained for various HRP-CN ^{1}H NMR data sets; (3) the predicted dipolar shifts for all protons in HRP-CN for both structurally conserved and variable active site residues correlate well with observed values; (4) the magnetic axes determined for HRP-CN provide an interpretive model for the strong but selective influence on shifts for HRP-CN upon the binding of the substrate[15] benzhydroxamic acid, BHA; and (5) the model serves as a basis for interpreting the variable hyperfine shifted pattern for the variety of NMR characterized cyanide-inhibited classical heme peroxidases.[8-14] The needed extensive and definitive assignments for HRP-CN have been reported,[9,10] as has the influence of BHA binding on the resolved resonances.[15c] The effect of BHA on the unresolved resonances will be pursued by 2D NMR.

(9) de Ropp, J. S.; Yu, L. P.; La Mar, G. N. *J. Biomolec. NMR* **1991**, *1*, 175-192. Sette, M.; de Ropp, J. S.; Hernandez, G.; La Mar, G. N. *J. Am. Chem. Soc.* **1993**, *115*, 5237-5245.

(10) Chen, Z.; de Ropp, J. S.; Hernandez, G.; La Mar, G. N. *J. Am. Chem. Soc.* **1994**, *116*, 8772-8783.

(11) Satterlee, J. D.; Erman, J. E. *Biochemistry* **1991**, *30*, 4398-4405. Satterlee, J. D.; Russell, D. J.; Erman, J. E. *Biochemistry* **1991**, *30*, 9072-9077.

(12) (a) de Ropp, J. S.; La Mar, G. N.; Wariishi, H.; Gold, M. H. *J. Biol. Chem.* **1991**, *266*, 5001-5008. (b) Banci, L.; Bertini, I.; Turano, P.; Tien, M.; Kirk, T. K. *Proc. Natl. Acad. Sci. U.S.A.* **1991**, *88*, 6956-6960. (c) Bertini, I.; Pease, E. A.; Tien, M.; Turano, P. *Biochemistry* **1992**, *31*, 10 009-10 017. (d) Banci, L.; Bertini, I.; Kuan, I. C.; Tien, M.; Turano, P.; Vila, A. J. *Biochemistry* **1993**, *32*, 13 483-134 89.

(13) Goff, H. M.; Gonzalez-Vergara, E.; Bird, M. R. *Biochemistry* **1985**, *24*, 1007-1013. Lukat, G. S.; Rodgers, K. R.; Jabro, M. N.; Goff, H. M. *Biochemistry* **1989**, *28*, 3338-3345. Dugad, L. B.; Wang, X.; Wang, C.-C.; Lukat, G. S.; Goff, H. M. *Biochemistry* **1992**, *31*, 1651-1655.

(14) (a) Veitch, N. C.; Williams, R. J. P.; Bray, R. C.; Burke, J. F.; Sanders, S. A.; Thorneley, R. N. F.; Smith, A. T. *Eur. J. Biochem.* **1992**, *207*, 521-531. (b) Satterlee, J. D.; Erman, J. E.; Mauro, J. M.; Kraut, J. *Biochemistry* **1990**, *29*, 8797-8804. (c) Banci, L.; Bertini, I.; Turano, P.; Ferrer, J. C.; Mauk, A. G. *Inorg. Chem.* **1991**, *30*, 4510-4516.

(15) (a) Morishima, I.; Ogawa, S. *J. Biol. Chem.* **1979**, *254*, 2814-2820. (b) Veitch, N. C.; Williams, R. J. P. In *Biochemical, Molecular and Physiological Aspects of Plant Peroxidases*; Lobarzewski, J., Greppin, H., Penel, C., Gaspar, T., Eds.; University of Geneva Press: Geneva, Switzerland, 1991; pp 99-109. (c) La Mar, G. N.; Hernandez, G.; de Ropp, J. S. *Biochemistry* **1992**, *31*, 9158-9168. (d) Veitch, N. C. In *Plant Peroxidases: Biochemistry and Physiology*; Welinder, K. G., Rasmussen, S. K., Penel, C., Greppin, H., Eds.; University of Geneva Press: Geneva, Switzerland, 1993; pp 56-64.

(16) Shulman, R. G.; Glarum, S. H.; Karplus, M. *J. Mol. Biol.* **1971**, *57*, 93-115.

(17) Emerson, S. D.; La Mar, G. N. *Biochemistry* **1990**, *29*, 1556-1566. Rajarathnam, K.; La Mar, G. N.; Chiu, M. L.; Sligar, S. G. *J. Am. Chem. Soc.* **1992**, *114*, 9048-9058. Rajarathnam, K.; Qin, J.; La Mar, G. N.; Chiu, M. L.; Sligar, S. G. *Biochemistry* **1993**, *32*, 5670-5680. Qin, J.; La Mar, G. N.; Ascoli, F.; Brunori, M. *J. Mol. Biol.* **1993**, *231*, 1009-1023. Qin, J.; La Mar, G. N.; Cutruzzola, F.; Allocatelli, C. T.; Brancaccio, A.; Brunori, M. *Biophys. J.* **1993**, *65*, 2178-2190.

(18) Morita, Y.; Funatsu, J.; Mikami, B. In *Peroxidases: Biochemistry and Physiology*; Welinder, K. G., Rasmussen, S. K., Penel, C., Greppin, H., Eds.; University of Geneva Press: Geneva, Switzerland, 1993; pp 1-4.

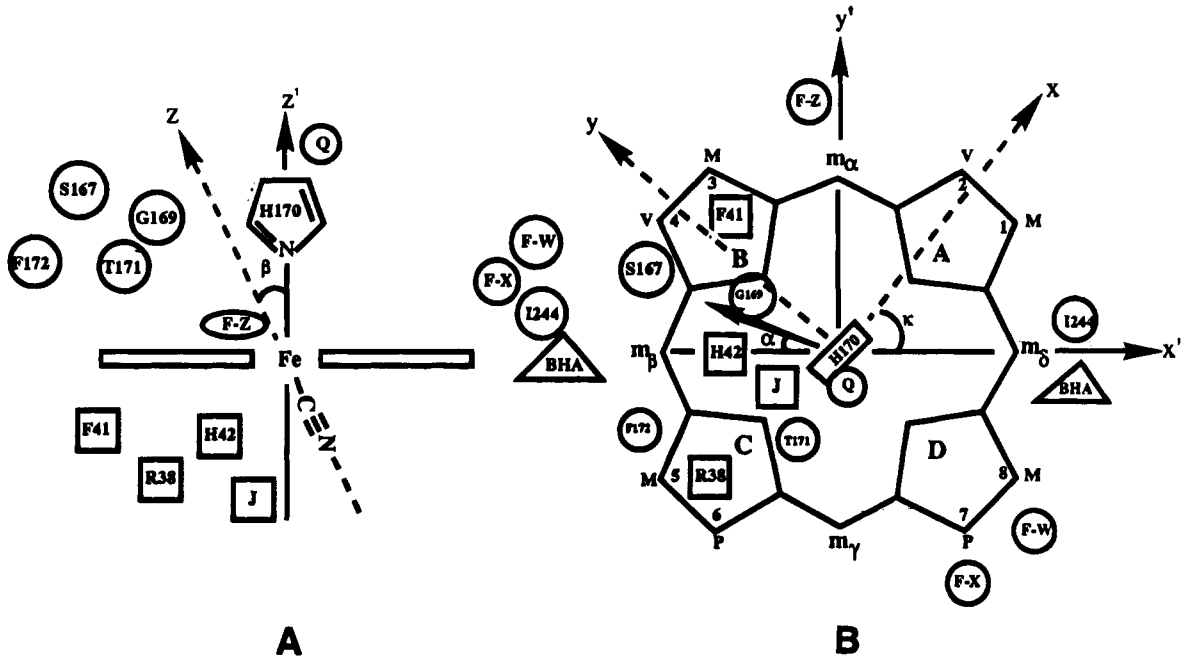

Figure 1. Schematic representation of the heme pocket structure of HRP: (A) edge-on view from the γ-meso direction, and (B) top view from the proximal side. The general positions of proximal (circles) and distal (squares) residues in the heme pocket, derived based on the crystal structure of CcP[3] and the previously reported NMR assignments of HRP-CN,[10] are labeled according to the HRP sequence. The residues F41, G169, T171, F172, and I244 were substituted from CcP to match the HRP sequence. The qualitative positions of several nonspecifically assigned residues, based on their NOE contact with either assigned residues and/or the heme, are also given in circles and labeled with letters. The general position of substrate BHA contact with the heme pocket is represented in triangle. The pseudosymmetry axes derived from the crystal structure of CcP are described by x', y', and z', with x',y' defined by the mean heme plane. A set of magnetic axes is defined by a coordinate system of x, y, and z. The β angle in (A) is the magnitude of the major magnetic or z-axis tilt from the heme normal (z' axis). The direction of the z-axis tilt is given by α, which is the angle between the projection of the tilted z-axis on the heme plane and the $-x'$ axis. The orientation for the rhombic axes x, y is described by κ which is the angle between the projection of x on the heme plane and the x' axis; for small β angle, $\kappa \sim \alpha + \gamma$.

Experimental Section

Sample Preparation. Isozyme C horseradish peroxidase, purity >98%, was purchased as a lyophilized powder from Boehringer Mannheim. NMR samples in ^2H_2O and ^1H_2O were 3 mM in protein, 30 mM in KCN at pH 7.0. Benzhydroxaminic acid, BHA, was titrated into a ^2H_2O solution of HRP-CN at 45 °C, pH 7.0, to form the tertiary substrate complex HRP-CN:BHA, as described in detail previously.[15c]

^{1}H NMR Spectra. All ^{1}H NMR spectra of HRP-CN in the presence of various amounts of BHA were recorded at 45 °C at 500 MHz on a GE Ω-500 spectrometer. 1D spectra were obtained over a spectral window of 40.0 kHz using 8192 data points with a 7.6-μs 90° pulse at a pulse repetition rate of 2 s^{-1}; exponential apodiziation introduced 5−10 Hz line broadening. 2D NOESY spectra[19] were collected using the method of States et al.,[20] with and without incorporating a WEFT pulse sequence[21] prior to the NOESY experiment, as detailed previously.[10] Data sets were collected in 512 blocks over 31.0 KHz using 1024 points, and a mixing time of 20 ms. The processing involved 30°-sine-bell-squared apodization prior to zero filling to 1024 × 1024 points and Fourier transformation. The spectra with 0.1, 0.4, and 10 molar equiv of BHA added to HRP-CN corresponded to 0.09, 0.39, and 1.0 mol fraction formation of the ternary substrate complex of HRP-CN:BHA as monitored by the averaged 8-CH_3 chemical shift.[15c] The peak positions for resolved resonances could be followed directly in the titration with BHA. Unresolved peaks could be followed by monitoring the position of the assigned NOESY cross peaks in pure HRP-CN with increasing BHA.

Magnetic Axes Determination. The magnetic axes were determined as described in detail elsewhere.[17] A computer least-squares search was carried out to minimize the error function, F/n:

$$F/n = \sum^{n}[\delta_{dip}(\text{obs}) - \delta_{dip}(\text{calc})R(\alpha,\beta,\gamma)]^2 \quad (2)$$

where δ_{dip}(calc) in the pseudosymmetry iron-centered coordinate system is given by eq 1, and the observed dipolar shift, δ_{dip}(obs), is given by:

$$\delta_{dip}(\text{obs}) = \delta_{DSS}(\text{obs}) - \delta_{DSS}(\text{dia}) \quad (3)$$

with δ_{DSS}(obs) the observed shift relative to DSS, and the δ_{DSS}(dia) the chemical shift of an isostructural diamagnetic complex. In the absence of such data, the latter is obtained via:

$$\delta_{DSS}(\text{dia}) = \delta(\text{sec}) + \delta(\text{rc}) \quad (4)$$

where δ(sec) and δ(rc) are the shifts from the residues including secondary structure effects,[22] and ring current effects,[23] respectively. The least-squares searches were carried out for three parameters to obtain the Euler angles, α, β, γ, using the magnetic anisotropy experimentally determined for the isoelectronic metMbCN,[17] $\Delta\chi_{ax} = 1.12 \times 10^{-33}$ m^{-3}, $\Delta\chi_{rh} = 0.37 \times 10^{-33}$ m^{-3}, or extended to five parameters to include determination of $\Delta\chi_{ax}$ and $\Delta\chi_{rh}$. In each case, the coordinates used for eqs 1 and 4 are those for the proximal helix backbone and the conserved distal His and Arg residues in the crystal structure of CcP-CN, converted to iron-centered pseudosymmetry coordinates where x', y' lie in the mean heme plane and pass through meso positions, with z' normal to the heme. Substitution of other amino acids in CcP to conform to the sequence of HRP was carried out by the Biosym Insight II program (Ala 174 → Gly 169, Ala 176 → Thr 171, etc.); for Trp 52 (CcP) → Phe 41 (HRP), the side chain orientation was used as determined[10] from the NOESY cross peaks to conserved nearby residues.

Dipolar Shift Simulations. Predictions of changes in dipolar shift with selective perturbations in the orientation of the major magnetic

(19) Macura, S.; Ernst, R. R. *Mol. Phys.* **1980**, *41*, 91−117.
(20) States, D. J.; Haberkorn, R. A.; Ruben, D. J. *J. Magn. Reson.* **1982**, *48*, 286−292.
(21) Patt, S. L.; Sykes, B. D. *J. Chem. Phys.* **1972**, *56*, 3182−3184. Lankhorst, P. P.; Wille, G.; van Boom, J. H.; Altona, C.; Haasnoot, C. A. G. *Nucl. Acids Res.* **1983**, *11*, 2839−2856.
(22) Wishart, D. S.; Sykes, B. D.; Richards, F. *J. Mol. Biol.* **1991**, *222*, 311−333.
(23) Cross, K. J.; Wright, P. E. *J. Magn. Reson.* **1985**, *64*, 220−231.

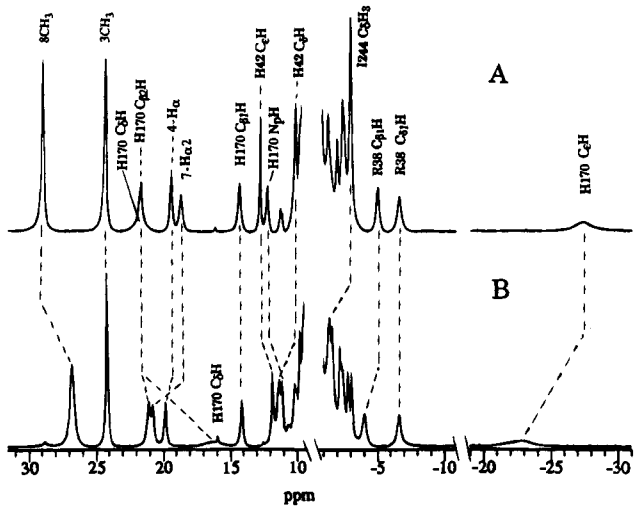

Figure 2. Resolved portions of the 500-MHz ^1H NMR spectra in ^2H_2O at 45 °C, pH 7.0, of (A) HRP-CN, and (B) the fully formed ternary substrate complex with BHA, HRP-CN:BHA; peaks are labeled based on the previously reported assignments.[15c]

axis were carried out by systematically varying the tilt (β), while keeping the direction of tilt (α) and rhombic axes ($\kappa \sim \alpha + \gamma$) constant, or by varying the direction of tilt (α) for constant tilt magnitude (β), and rhombic axes $\kappa \sim \alpha + \gamma$.

Results

Assignments in HRP-CN:BHA. The resolved portions of the 500 MHz ^1H NMR spectrum of HRP-CN in ^2H_2O at 45 °C, pH 7.0, are illustrated in Figure 2A, which are compared to those of the fully formed substrate-bound ternary complex, HRP-CN:BHA, for which the analogous spectral regions are shown in Figure 2B. The observed shifts of the resolved resonances in HRP-CN, δ_{DSS}(HRP-CN), and the changes in these shifts induced by BHA binding, as defined by:

$$\Delta\delta(\text{BHA}) = \delta_{DSS}(\text{HRP-CN:BHA}) - \delta_{DSS}(\text{HRP-CN}) \quad (5)$$

are listed in Table 1. The attenuation of the hyperfine shifts for all resonances in the HRP-CN:BHA complex compared to those in HRP-CN (with spectra shown in Figure 2), leads to severe spectral congestion in the unresolved portion of the 2D NOESY map for the fully formed substrate complex. However, since BHA exchange is rapid on the NMR time scale at 45 °C, the important cross peaks previously reported[10] for HRP-CN could be followed upon only partial saturation of the BHA binding site. The chemical shifts for the fully formed substrate complex, δ_{DSS} (HRP-CN:BHA), were obtained from shifts of only partially (9.0%, 39.5%) formed complex by adjusting for the mole fraction of substrate-bound complex. The mole fraction substrate bound complex was readily obtained[15c] from the observed chemical shift of the resolved, averaged 8-CH_3. The majority of the resonances of interest in HRP-CN:BHA could be located[24] (not shown; see supplementary material).

Magnetic Axes Determination. Definitively assigned proton signals for noncoordinated residue protons in HRP-CN,[10] whose coordinates relative to C*c*P may be considered highly conserved in HRP, are the backbone (NH, $C_\alpha H$) of the proximal helix for residues Gly 169-Phe 172 (5C_αHs, 4NH),[25] the complete Arg 38 system (NH, 7 CHs), and six His 42 signals (2 CH, 2 NH for the ring, the NH, $C_\alpha H$) (HRP labeling). The 23 data points available comprise the largest input data set **A**(23); because of large uncertainties in the His 42 ring NH diamagnetic shift, the $N_\epsilon H$, $N_\delta H$ signals are omitted in the data set **B**(21). The 15 point set **C**(15) retains only the signals with significant dipolar shifts, the proximal backbone for Gly 169, His 170 (5), the complete Arg 38 (8), and the ring nonlabile protons of His 42 (2). The available assignments for C*c*P-CN[11] are neither as complete nor definitive as for HRP-CN, in part because the reduced protein stability requires working at lower temperature

(24) The intense signal from the excess BHA needed to induce significant substrate-bound complex resulted in t_1 streaks in the NOESY map that obscure some of the weakly relaxed signals in the aromatic window.

(25) While His 170 is coordinated to the iron and its signals will exhibit both contact and dipolar shift, extensive studies of metMbCN complexes have shown[17] that the contact contribution is negligible for $C_\alpha H$ and N_pH.

Table 1. ^1H NMR Shifts for HRP-CN and Its Ternary Substrate Complex with Benzhydroxamine Acid

		HRP-CN			
residue	proton	δ_{DSS}(obs)[a] (ppm)	Curie slope[b] (ppm·K × 10^3)	δ_{DSS}(dia)[c] ppm	$\Delta\delta_{(BHA)}$[d] ppm
Arg 38	N_pH	5.67	−0.8	8.45	0.31
	$C_\alpha H$	0.59	−1.0	3.36	0.85
	$C_{\beta 1}H$	−4.91	−2.4	1.80[e]	0.78[e]
	$C_{\beta 2}H$	−0.59	−0.4	1.54[e]	0.44
	$C_{\gamma 1}H$	0.61	1.4	−0.11	0.74
	$C_{\gamma 2}H$	−1.40	0.7	−1.77	1.37
	$C_{\delta 1}H$	−6.56	−2.0	0.44	−0.18[e]
	$C_{\delta 2}H$	1.02	0.6	2.37	−0.54
His 42	NpH	9.09	0.9	6.99	0.70
	$C_\alpha H$	4.76	0.8	2.59	*f*
	$C_\delta H$	10.03	2.1	3.42	1.37
	$N_\delta H$	16.08	1.8	11.13	−0.1[e]
	$C_\epsilon H$	12.70	2.3	6.95	−0.93[e]
	$N_\epsilon H$	29.78	11.0	9.17	−1.0[e]
Gly 169	N_pH	10.12	1.9	7.54	−0.62
	$C_{\alpha 2}H$	5.73	1.7	3.63	−0.93
	$C_{\alpha 1}H$	4.99	1.0	3.33	−0.75
His 170	N_pH	12.16	3.0	5.60	−1.19[e]
	$C_\alpha H$	9.49	3.4	0.38	−0.91
	$C_{\beta 1}H$	21.44	8.9	−1.34	−0.28[e]
	$C_{\beta 2}H$	14.18	4.9	−4.28	0[e]
	$C_\delta H$	21.7	11.0	−0.53	−5.1[e]
	$C_\epsilon H$	−27.4	−9.8	0.69	5.0[e]
Phe 41	$C_\delta Hs$	7.62	0.7	5.73	1.48
	$C_\epsilon Hs$	6.34	0.9	4.92	*f*
	$C_{\beta 2}H$	2.65	−0.3	3.49	*f*
Ile 244	$C_\gamma H$	0.21	−0.2	0.79	0.18
	$C_\gamma H$	1.17	−0.3	0.95	*f*
	$C_\delta H_3$	−2.87	−1.6	0.28	1.22
Thr 171	N_pH	9.05	4.8	7.27	*f*
	$C_\alpha H$	5.04	3.3	3.68	*f*
Phe 172	N_pH	9.49	1.1	7.66	*f*
	$C_\alpha H$	5.65	0.4	4.21	*f*
Phe 152 (?)	$C_\delta Hs$ or $C_\zeta H$	7.15	−0.2	7.72 or 8.23	−0
	$C_\eta Hs$	6.25	−0.6	7.99	−0
	$C_\zeta H$ or $C_\delta Hs$	5.44	−0.8	8.23 or 7.72	−0
Ser 167	$C_\alpha H$	5.73	1.2	3.13	−0
	$C_\beta H$	3.26	1.6	3.57 or 3.36	*f*
Phe-W	ring-Hs	7.73	0.0		
Phe-X	$C_\delta Hs$ or $C_\zeta H$	4.77	−1.4		0.10
	$C_\epsilon Hs$	6.37	−0.7		*f*
	$C_\zeta H$ or $C_\delta Hs$	6.97	−0.3		*f*
Q	Q-1	8.87	2.0		~0
	Q-2	8.32	1.5		~0
	Q-3	6.59	0.9		~0
	Q-4	5.10	0.3		~0
J	J-1	6.41	1.2		*f*
	J-2	3.27	0.7		*f*

[a] Shifts at 45 °C, in ^2H_2O (except for His 42 $N_\epsilon H$, $N_\delta H$), referenced to DSS, taken from ref 10. [b] Slope in a Curie plot, i.e., plot δ_{DSS}(obs) versus reciprocal absolute temperature, taken from ref 10. [c] Chemical shift, relative to DSS, for analogous dimagnetic complex, as calculated via eq 4 in the C*c*P-CN crystal structure. [d] Change in shift for HRP-CN upon forming ternary complex with BHA, as given by eq 5. [e] Taken from ref 15c. [f] Signals not identified in HRP-CN:BHA due to spectral congestion.

Table 2. Orientation of the Magnetic Axes in HRP-CN and CcP-CN

NMR data	input data set[a]	no. parameter	Euler angles, deg α	β	γ	κ	magnetic anisotropies $\Delta\chi_{ax}$ ($\times 10^{33}$ m^{-3})	$\Delta\chi_{rh}$ ($\times 10^{33}$ m^{-3})	error function F/n ppm^2
HRP-CN	**A(23)**	3	−10	20.6	60	50	1.11[b]	0.37[b]	1.18
	A(23)	5	−15	20.6	65	50	1.02	0.54	0.94
	B(21)	3	−10	20.9	60	50	1.11[b]	0.37[b]	1.13
	B(21)	5	−15	21.2	65	50	0.90	0.56	0.32
	C(15)	5	−20	23.2	70	50	0.90	0.60	0.20
HRP-BHA	**C(15)**	3	−10	14.8	60	50	0.90	0.60	0.37
CcP-CN	**D(19)**	3	−30	19.2	90	60	1.11[b]	0.37[b]	3.08
	D(19)	5	−25	20.2	80	55	0.94	0.52	2.04
	E(14)	3	−20	21.8	90	70	1.11[b]	0.37[b]	2.70
	E(14)	5	−25	21.4	80	55	0.98	0.56	1.50

[a] Data sets as defined in text. [b] Data for metMbCN taken from ref 17.

with the increase in linewidth complicating 2D experiments. The 19 dipolar shifted signals for which assignments have been proposed[11,26] for CcP-CN are for the distal Arg 48 (5) and His 52 (4), the proximal His 175 (2), Ala 174 (3), and Leu 232 (3), and one each for Ala 176 and Trp 51, which comprise the largest data set **E**(19); a smaller set **F**(14) omits the His 52 labile protons and the less definitively identified Ala 174 signals. In each case, the iron-centered coordinates to obtain the geometric factors in eq 1 and δ_{DSS}(dia) in eq 4 were obtained from the CcP-CN crystal structure.[3] Limited investigation of the LiP[6] crystal coordinates[6,27] were also carried out for the HRP-CN ^{1}H NMR data.

Representative results of both three- and five-parameter searches for the variety of HRP-CN ^{1}H NMR input data[10] and the CcP-CN crystal coordinates[3] are listed in Table 2. The resulting Euler angles are relatively insensitive to the data base. In each case, the extension of the three-parameter search to include the anisotropies led to an improved fit with minimal change in the angles, with the axial anisotropy reduced compared to that determined for metMbCN.[17] The range in the individual Euler angles with variable input sets for HRP-CN are 10° for α, 2.6° for β (Table 2), and their relative ranges likely reflect their relative uncertanties in the values of the angles.[17] The high quality of the five-parameter fit for HRP-CN based on input data set **B** is dramatically illustrated in Figure 3, which plots the δ_{dip}(obs) against δ_{dip}(calc). Not only is there an excellent correlation between the observed and calculated δ_{dip} for the 21 input data, but the His 42 N_δH, N_ϵH shifts not used in the fit are also well predicted. The most complete assignments[24] for the fully formed HRP-CN:BHA allow only the use of the 15-member data set **C**, for which a three parameter search, using the $\Delta\chi$s obtained from HRP-CN, leads to the Euler angles listed in Table 2. Comparison of the Euler angles for the same input data sets **C** for HRP-CN and HRP-CN:BHA indicates that β has decreased by ~9°, α has become more negative by 10°, and $\kappa = \alpha + \gamma$ has not changed. The change in α is comparable to the range of α obtained from different input data, and may not be significant. The change in β, however, is larger than the range with different input data, and is likely the origin of the large spectral perturbations (see Discussion).

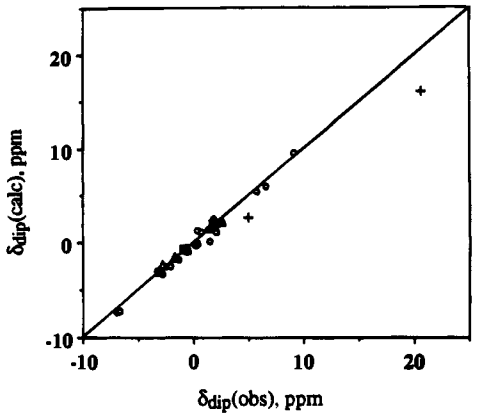

Figure 3. Plot of observed dipolar shift, δ_{dip}(obs), versus calculated dipolar shift, δ_{dip}(calc), obtained using the parameters reported in Table 2 for data set B(21) in a five-parameter fit: (open circle) resonances used as input; (+ sign) N_δH and N_ϵH of H42; (solid square) C_δHs and $C_{\beta 2}$H of F41; (solid triangle) S167 C_αH; (open triangle) F-Z ring protons; and (solid circle) $C_\delta H_3$, C_γH, and $C_{\gamma'}$H of I244. The solid line represents the ideal correlation.

The results of three- and five-parameter least-squares fits for CcP-CN NMR data[11,26] using the CcP-CN crystal coordinates[3] are given at the bottom of Table 2. The four searches again yield very similar Euler angles, with the anisotropies from the five-parameter searches very comparable to those obtained for HRP-CN above. For the more reliable data set **E**, the δ_{dip}(obs) correlate well with the δ_{dip}(calc), with nodal surface well-defined (correct signs for all shifts). The somewhat larger residual error function for CcP-CN, when compared to HRP-CN, likely arises from ambiguities in the distal Arg assignments which could not be established by scalar correlation (see supplementary material).[11] It is noted that the orientation of the magnetic axes using HRP-CN and CcP-CN ^{1}H NMR data are remarkably similar.

The slope of δ_{dip}(obs) with respect to reciprocal temperature in a Curie plot, as given in Table 1, has been shown to be directly proportional to the magnitude of δ_{dip} in a variety of metMbCN complexes,[17] as long as a residue does not exhibit changes in orientation with temperature. A plot of the variable-temperature slope versus the δ_{dip}(obs) for HRP-CN is illustrated in Figure 4. The excellent correlation not only serves as confirmation for the experimental dipolar shift for assigned residues, but confirms a structurally invariant pocket over the temperature range studied.

Systemic Perturbation of the Magnetic Axes. The influence of variable extents of tilt (β) and direction (α) for the major

(26) The chemical shifts (at 23 °C) used for the CcP-CN are: Arg 48, N_pH 7.18, C_βHs −3.99 and −3.28, C_δHs −4.66 and −1.2; Trp 51, 1NH (labeled HE1 in CcP crystal structure) 18.0; His 52, C_δH 9.6, N_δH 16.4, C_ϵH 14.0, N_ϵH 28.6; Ala 17, N_pH 10.0, C_αH 2.65, $C_\beta H_3$ 0.3; Ala 176, N_pH 6.99; His 175, N_pH 12.0, CαH 8.48, C_βHs 19.5 and 14.9; Leu 232, $C_\delta H_3$s −2.78 and −1.24, C_γH 0.70, as taken from ref 11.

(27) The use of the LiP crystal coordinates resulted in similarly reasonable correlations of δ_{dip}(obs) with δ_{dip}(calc) for magnetic axes with slightly smaller tilt (β ~17°) and in a similar direction (toward the δ-meso). The difference in β may result largely from the definition of the symmetry-coordinate system, as the heme is not planar in either CcP[3,4] or LiP.[6] The CcP coordinates were favored over the LiP coordinates for two reasons. The HRP-CN electronic structure, as reflected in the ^{1}H NMR spectra, much more closely resembles that of CcP-CN[11] than LiP-CN.[12a,b] Moreover, the crystal structure of CcP[3,4] shows that the axial His imidazole is oriented close to the N−Fe−N vector for pyrroles A and C, which is consistent with the large low-field heme 3-CH_3, 8-CH_3 contact shifts at both CcP-CN[11] and HRP-CN.[8,9] The crystal structure of LiP[6] has the axial His imidazole aligned closer to a meso-Fe-meso axis, which is consistent with the smaller low-field 3-CH_3, 8-CH_3 shifts in LiP-CN.[12a,b]

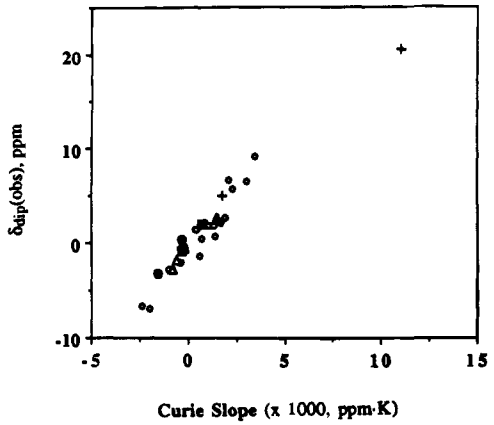

Figure 4. Observed dipolar shifts, δ_{dip}(obs), as a function of the slope of the Curie plots $d\delta_{obs}(DSS)/d(1/T)$, for resonances (open circle) of data set B(21) reported in Table 2: (+ sign) $N_\delta H$ and $N_\epsilon H$ of H42; (solid squares) $C_\delta Hs$ and $C_{\beta 2}H$ of F41; (solid triangles) S167 $C_\alpha H$; (open triangles) F-Z ring protons; and (solid circles) $C_\delta H_3$, $C_\gamma H$, and $C_{\gamma'}H$ of I244.

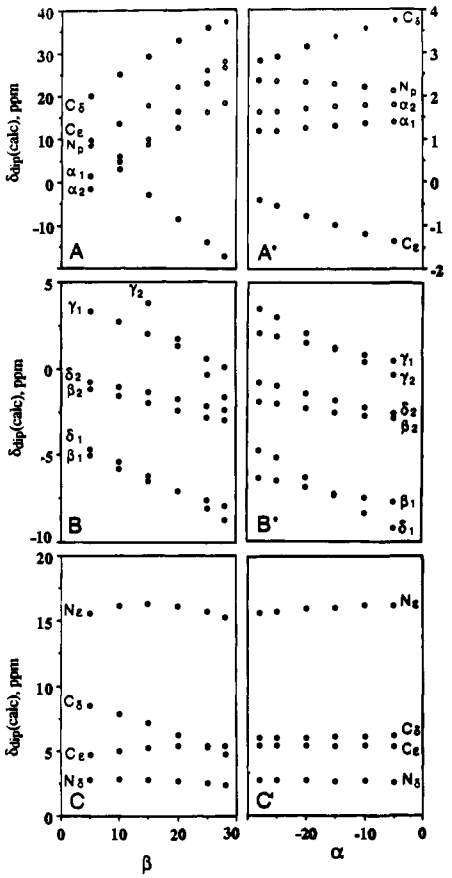

Figure 5. Calculated dipolar shifts, δ_{dip}(calc), as a function of β for fixed α and κ ($\alpha + \gamma$), **A-C** and as a function of α for fixed β and κ ($\sim\alpha + \gamma$), (**A'-C'**) determined from the five-parameter fit using data set B(21) for HRP-CN. The resonance plotted are Gly 169 and His 170, (**A, A'**), distal Arg 38 (**B, B'**), and distal His 42 (**C, C'**). Note the different vertical scales for His 170 (left) and Gly 169 (right) in **A** and **A'**.

magnetic axis, z, on the well-resolved dipolar shifted signals of HRP-CN was assessed. δ_{dip}(calc) values for Gly 169, His 170, Arg 38, and His 42, upon variation in β (tilt) for fixed α, γ (fixed orientation of tilt, fixed rhombic axes), are plotted in Figure 5, A, B, and C, respectively, and upon variations in α (direction of tilt) with fixed β (tilt) and $\kappa = \alpha+\gamma$ (rhombic axes), are shown in Figure 5, A', B', and C', respectively. The

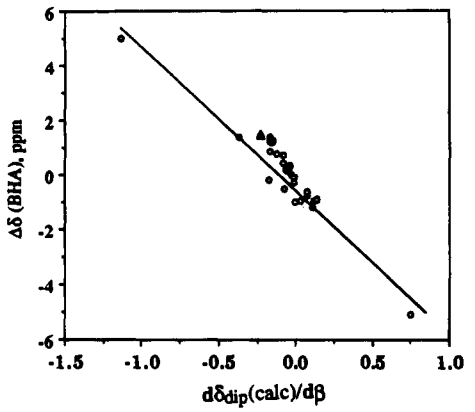

Figure 6. Chemical shift differences between HRP-CN:BHA and HRP-CN, $\Delta\delta$(BHA), at 45 °C, as a function of the calculated dipolar shift gradients with β angle of the magnetic axis, $d\delta_{dip}(calc)/d\beta$: (open circles), resonances sequence specifically assigned; (solid circles) $C_\delta H_3$ and $C_\gamma H$ of I244; (open triangles) F41 $C_\delta Hs$. The solid line is the best fit to a straight line over the specifically assigned resonances.

variations are centered on the α, β values determined for HRP-CN. It is clear that these perturbations of the orientation of the major magnetic axis make detailed and selective predictions as to the direction and magnitude of *expected dipolar shift changes*.

Over the range of the largest shifts observed[15c] upon BHA binding (for the ring of His 170), the slope of the plots in Figure 5 are approximately linear (with the exception of His 42 $N_\epsilon H$; see Figure 5C). The sensitivity to the selective change in β for HRP-CN can be expressed by the slope of the plot in Figure 5, $d\delta_{dip}(calc)/d\beta$, which is plotted in Figure 6 against the change in observed shift in HRP-CN induced by complete binding of BHA, i.e., $\Delta\delta$(BHA) (eq 5); a good correlation is observed for all nonheme resonances.[28] Changes in only α generally predict insignificant changes in δ_{dip} for many of the resonances, in contrast to the significant shift change observed upon BHA binding[29] (not shown; see supplementary material). The influence of variable orientation of the major magnetic axis for fixed anisotropies and rhombic axes on the axial His 170 imidazole ring $C_\delta H$, $C_\epsilon H$ was explored over a more complete range of orientation of the major magnetic axis. The predicted dipolar shifts, as a function of both β and α for fixed rhombic axes, $\kappa \sim \alpha + \gamma$, are represented in the circular plot in Figure 7.

Discussion

Orientation of the Magnetic Axes. The magnetic axes for C*c*P-CN, as deduced from the limited available C*c*P-CN ^1H NMR data,[11,26] provide a reasonable quantitative representation for the hyperfine shifts of noncoordinated residues (see supplementary material). The rhombic axes for the five-parameter fits, $\kappa \sim \alpha + \gamma = 55°$, coincide approximately with the orientation of the axial His imidazole with respect to the heme[3] (Figure 1B), as also found in metMbCN complexes.[17] The major magnetic or z axis is found tilted (~20°) from the heme normal toward the β-meso-H (or the magnetic -z axis toward the δ-meso-H; see Figure 1B), which is approximately colinear

(28) BHA binding induces large shifts for heme 8-CH_3 ($\Delta\delta$(BHA) = −2.2 ppm) and $7H_\alpha$ ($\Delta\delta$(BHA) = 2.1 ppm), which are most likely due to ring current effects of BHA and slight reorientation for the propionate group, both of which interact with BHA.[15c] The other positions, 1-CH_3, 3-CH_3, 5-CH_3, and the meso-Hs, show small upfield shifts (~0.2 ± 0.1 ppm), which are consistent with small predicted upfield shift changes due to decreased tilt.

(29) In particular, a change in β for fixed κ predicts shift changes in the same direction for all three Gly 169 protons (Figure 5A), as is observed. Varying solely α predicts shifts in opposite direction for N_pH and $C_\alpha Hs$ (Figure 5A').

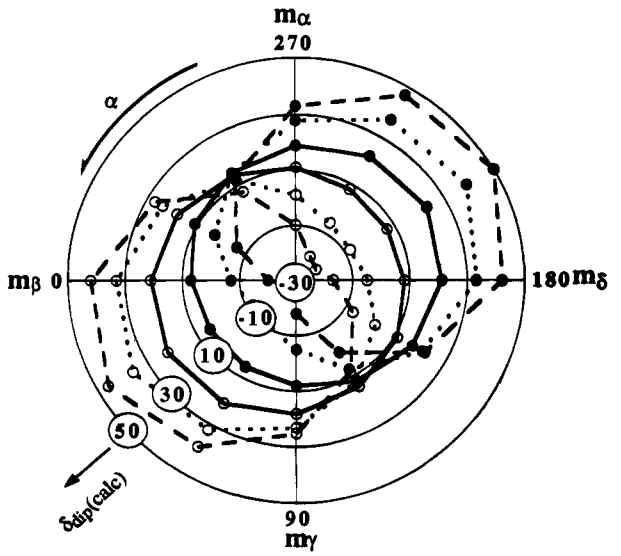

Figure 7. Plot of δ_{dip}(calc) for the axial His $C_\delta H$ (open circles) and $C_\epsilon H$ (filled circles) in HRP-CN as a function of tilt, β (in the range 5−25°), and direction of tilt, α (0→360°) for fixed rhombic axes $\kappa \sim \alpha + \gamma$, using the anisotropies and rhombic axes determined in the five-parameter fit with 21 points input data set B: (—) $\beta = 5°$, (···) $\beta = 15°$, and (- - -) $\beta = 25°$. The meso positions on the heme plane are identified as $m_\alpha \rightarrow m_\delta$. The chemical shift scale is radial, with the center at −30 ppm to +50 ppm at the periphery of the circular plot.

with the apparent orientation of the Fe-CN vector revealed in the X-ray crystal structure of C*c*P-CN.[3] A direct correlation between orientation of the major magnetic axis and Fe-CN tilt has been observed in several metMbCN complexes.[17] It appears that the major magnetic axis reflect tilt of the Fe-CN unit in C*c*P-CN (and presumably other heme peroxidases; see below) as well. Hence, condition no. 1 for the validity of our approach is satisfied.

The magnetic axes for HRP-CN determined on the basis of the C*c*P-CN crystal coordinates for the proximal helix backbone and the conserved distal His 42 and Arg 38 predict the dipolar shift surprisingly well (Figure 3), and the orientation of the axes is remarkably insensitive to the exact selection of the ^{1}H NMR input data (Table 2). Hence, condition 2 for our approach is validated. The nodal surface (sign of dipolar shifts) is particularly well defined for protons distributed over the whole heme cavity. The ability to generate a set of magnetic axes which can reproduce the shifts so well provides indirect support for the conserved structure of the pocket of HRP-CN when compared to C*c*P-CN. The latter conclusion had been reached independently on the basis of NOE and NOESY data on HRP-CN.[9,10] The axial magnetic anisotropy for either HRP-CN or C*c*P-CN determined from the five-parameter least-squares searches is somewhat smaller (0.90×10^{-33} m^{-3}) than that previously determined for metMbCN[17] (1.1×10^{-33} m^{-3}), which is consistent with the observed reduction in the *g*-tensor anisotropy in HRP-CN[30,31] relative to metMbCN.[32] The excellent representation of the dipolar shift nodal surface and the reduced anisotropy confirm condition 3 for this approach.

The magnetic axes for HRP-CN are similar to those obtained for C*c*P-CN; a tilt of ~20° from the heme normal toward the β-meso, with rhombic axes along a N−Fe−N vector. Since the tilt magnitude and direction correlate with Fe-CN tilt in C*c*P-CN,[3] we make the reasonable assumption that the *z* axis coincides to the Fe-CN tilt in HRP-CN (the Fe-CN tilt actually corresponds to the -*z* axis; see Figure 1A). The orientation of the major magnetic axis does not indicate whether the Fe-CN unit is just tilted or also bent, since the magnetic properties likely reflect the Fe−C vector.[17] Recent resonance Raman studies on HRP-CN have shown[33] that there are present two types of Fe-CN units, one of which is significantly bent; these two Fe-CN forms are completely time-averaged on the NMR time scale. The tilt of the Fe-CN unit from the heme in C*c*P-CN and HRP-CN likely results from the strong hydrogen bonding with the protonated distal His ring, as directly detected by ^{1}H NMR in HRP-CN.[8d] This hydrogen bond provides an important link between the distal proximal pockets which links the acid−base properties in the distal and proximal His.[1,4,8d,30,33]

Assignments for the hyperfine shifted signals of the $C_\alpha H$ of Ser 167 (Met 172 in C*c*P) and $C_{\beta 2} H$ of Phe 41 (Trp 52 in C*c*P) in HRP-CN were proposed[10] on the basis of a highly conserved NOESY cross peak pattern when compared to the crystal structure of C*c*P. The side chain of Phe 41 was also located[10] and its orientation estimated on the basis of NOE patterns to the adjacent Arg 38, His 42, and heme 3-CH_3. We note that the δ_{dip}(obs) for all of these protons show an excellent correlation with δ_{dip}(calc), as shown in Figure 3. A CH_2CH_3 fragment of a proximal Ile has been observed[9,10] in HRP-CN with strong dipolar contact with the pyrrole A, D junction and the axial His 170 ring. Sequence homology to C*c*P has led to the proposed origin[14a] as Ile 244 in HRP (Leu 232 in C*c*P). The assignments to Ile 244 in HRP-CN is supported by noting the excellent correlation in Figure 3 between the observed and predicted dipolar shift for Leu 232 (C*c*P) → Ile 244 (HRP). Molecular modeling studies of HRP indicate that Ile 180 near the heme 8-CH_3 is an alternate possibility.[34] The present NMR data only confirm that the Ile CH_2CH_3 fragment in HRP occupies a position very similar to that held by Leu 232 in C*c*P.

Similarly, a Phe side chain in contact with the junction of pyrrole A and B appears homologous[2] to Phe 158 in C*c*P[3] and has been attributed[14a] to Phe 152 in HRP. Again, the good agreement between predicted and observed δ_{dip} in Figure 3 strongly supports its conserved position in the active site. One additional Phe side chain with upfield hyperfine shift of ~−1 to −2 ppm has been located[10] in contact with the 7-propionate $C_\alpha H_2$ (designated Phe X in Figure 1). The sequence origin has not been identified because of the low homology to C*c*P and the large number of Phe in the vicinity.[2] However, the dipolar shift for the proximal Thr 180 of C*c*P in contact with this propionate is predicted to exhibit similar −1 to −2 ppm dipolar shift. The good correlation of δ_{dip}(obs) and δ_{dip}(calc) for the HRP-CN signal of Ser 167, Phe 41, Ile 244, and Phe 152 provides additional evidence for both the conserved disposition for these residues with respect to C*c*P, and for the validity of the magnetic axis of HRP-CN. These results further support condition 3 for our interpretive model.

Lastly, parts of two residues, designated residues Q and J, were located[10] in HRP-CN which exhibit dipolar contact with the proximal and distal His, respectively. Residue Q is in contact with the His 170 C_βHs, a position occupied by Phe 202 in C*c*P[3] and Phe 204 in LiP.[6] Using the correlation between Curie slope and δ_{dip}(obs) in Figure 3, the Curie slopes for Q1, Q2 in Table 1 indicate dipolar shifts of 3 to 4 ppm. Sequence homology between HRP and C*c*P for this segment is low, but

(30) Blumberg, W.; Peisach, J.; Wittenberg, B. A.; Wittenberg, J. B. *J. Biol. Chem.* **1968**, *243*, 1854−1862.

(31) The relative magnitude of the anisotropies for HRP-CN, $\Delta\chi_{ax}$:$\Delta\chi_{rh}$ ~ 3:2, corresponds well with the ratio of theoretical values, $g_{zz}^2 - {}^1/_2(g_{xx}^2 + g_{yy}^2)$ and $g_{xx}^2 - g_{yy}^2$, obtained for the low-temperature EPR spectra,[30] *g* ~ 3.0, 2.1, 1.2.

(32) Hori, H. *Biochim. Biophys. Acta* **1971**, *251*, 227−235.

(33) Al-Mustafa, J.; Kincaid, J. R. *Biochemistry* **1994**, *33*, 2191−2197.

(34) Loew, G. H. In *NMR of Paramagnetic Macromolecules*; La Mar, G. N., Ed.; Kluwer Academic Publishers, in press.

the relevant portion of the former protein does not contain a Phe.[2,34] The δ_{dip}(calc) values for Phe 202 in CcP are 2−3 ppm, which are similar to those deduced for Q. Residue J in contact with the distal His 42 ring[10] also occupies a position for which there is little sequence homology[2] between CcP and HRP. Again, the Curie slopes for the protons indicate (Table 1, Figure 4) dipolar shift of 1 to 2 ppm, which are consistent with the calculated 1 to 2 ppm values for two protons in CcP which are close to the distal His ring (Leu 144 $C_\delta H_3$, 1.8 ppm; Asn 82 $C_\alpha H$, 1.6 ppm). When more extensive 2D NMR studies on HRP-CN identify the sequence origin of residues Q and J, the δ_{dip}(obs) will aid in quantitatively placing these residues in the heme pocket, as has been reported in metMbCN complexes.[17]

The previous 2D NMR studies of HRP-CN had identified all protons in the heme cavity <6.5Å from the iron,[8-10] as deduced from sequence homology to CcP and the crystal structure of the latter protein, except for the side chain labile protons of the distal Arg. The presently determined magnetic axes for both CcP-CN and HRP-CN predict[35] that up to three of the guanidyl protons should be resolved in the low-field window near 12 and 15 ppm. Previous NMR studies on HRP-CN in ^1H_2O, however, had shown[8d] that the only hyperfine shifted labile protons which are detectable in the low-field region arise from His 42 and His 170. The failure to observe the hyperfine shifted guanidyl proton is more likely due to rapid exchange with water. The relatively rapid exchange of the distal His 42 labile protons has demonstrated the facile access of solvent into the distal cavity.[36]

Influence of Benzhydroxamic Acid Binding. BHA binds more strongly than other substrates of HRP,[37] and is unique in inducing significant perturbation of the positions of hyperfine shifted signals for HRP-CN.[15,38] The selective sensitivity of shifts has been interpreted to reflect proximity of the affected residue to the substrate binding site.[15b] The magnetic axes determined directly for HRP-CN:BHA indicate comparable changes in α and β from those for HRP-CN (Table 2). However, the uncertainty in β is significantly smaller than in α (or κ), as reflected in the sensitivity of the angles to the use of different input data. Hence this implies that BHA more likely significantly influences β than α. The good correlation between the magnitude of the BHA induced shifts, $\Delta\delta$(BHA), and the predicted gradients of the dipolar shift with decrease in β (Figure 6) strongly supports both the notion that the shift perturbations result from a change in magnetic axes, and that they change result predominantly from a decrease in the tilt (β) of the Fe-CN unit by ~9°. The binding of the aromatic ring of BHA both in HRP and HRP-CN has been to shown[15b-d,38,39] to occur near pyrrole D, as evidenced by NOEs between 8-CH_3, 7Hα, and BHA, with the side chain extended into the distal pocket toward His 42, to which an NOE is also observed in HRP-CN.[15b,c] Other substrates bind near the same site at the heme periphery, as evidenced by the formation of heme δ-meso substituents in suicide inhibition studies,[40] but do not have side chains which extend as far into the distal cavity as BHA. BHA binds at a site at the heme periphery toward which the Fe-CN unit is tilted in HRP-CN[15c] (see Figure 1B). Hence it is reasonable that BHA binding opposes or lessens this tilt.

Several conclusions can be drawn from the analysis of BHA binding. The good correlation of BHA-induced shifts with predicted shift changes with magnetic axis validates condition 4 of our proposed approach. The correlation of the BHA-induced shifts with changes in tilt of the magnetic axes (Fe-CN unit) dictates that the shift change for a given proton in the heme pocket does not reflect its proximity to the substrate binding site. The likely explanation that numerous smaller aromatic substrates do not induce significant shift changes in the ^1H NMR spectrum of HRP-CN[14a,15a,b,18] is that the substrates do not extend far enough into the distal pocket to influence the Fe-CN tilt. It has been observed by resonance Raman spectroscopy that the binding of the substrate BHA influences the Fe-CO tilt in reduced HRP-CO.[41] A similar study of the influence of BHA on Fe-CN tilt in HRP-CN has not yet been reported.

Comparison to Other Cyanide Inhibited Heme Peroxidases. The ^1H NMR spectra of HRP-CN and CcP-CN share many similarities in both the heme contact shift and the noncoordinated residue dipolar shift patterns.[8-11] The very similar orientation of their magnetic axes are clearly responsible. The hyperfine shift patterns, particulary for nonheme resonances, are also pairwise similar[12] for LiP-CN and MnP-CN, each of which is distinct from that displayed by HRP-CN and CcP-CN.[8-11] This differential sensitivity of the *structurally conserved residues to* the genetic origin of the protein has a ready explanation in our model for the hyperfine shift pattern in terms of the tilt of the Fe-CN unit. The simulations in Figure 5 are relevant to this argument. While the simulations in Figure 5 give only the dipolar shifts, *changes* in shifts with genetic origin of the protein for the structurally conserved axial His and distal catalytic Arg and His should correlate with changes in predicted dipolar shift.

The salient differences between the resonance positions of the axial His and distal Arg and His in HRP-CN/CcP-CN[10,11] → LiP-CN/MnP-CN[12] are: low-field bias by 20 ppm of $C_\epsilon H$, and upfield bias of ≥15 ppm for $C_\delta H$ for the axial ligated His, low-field bias by ≥5 ppm for $C_{\delta 1}H$, $C_{\beta 1}H$ of the distal Arg,[42] and essentially unchanged shifts for the distal His ring.[43] These are precisely the dipolar shift changes predicted in Figure 5 upon decreasing β for 20° in the former to ~5° in the latter peroxidase complexes. This leads to the proposal that LiP-CN and MnP-CN exhibit significantly less tilt of the major magnetic axis (or the Fe-CN unit) from the heme normal when compared to HRP-CN and CcP-CN. In particular, this direct correlation between the predicted patterns of the distal Arg/His and axial His hyperfine shifts based on variable tilt of the magnetic axes validates condition 5 of our interpretive model of the NMR spectra for cyanide-inhibited heme peroxidases.

(35) The magnetic axes and anisotropies for the five-parameter search for HRP-CN based on the 21 data set input predicts δ_{dip} shifts of 11.8 ppm for $N_\epsilon H$, and 6.3, 2.8 ppm for the $N_\eta H_2$ which is closer to the iron in CcP-CN; the only other $N_\eta H_2$ is predicted to have negligible dipolar shifts (<1 ppm). When δ_{DSS}(rc) is taken into consideration, the $N_\epsilon H$ should resonate near 15 ppm from DSS, and the $N_\eta H_2$ at 9 and 12 ppm. Even with significant uncertainties to the estimated δ_{dip}(calc), at least the $N_\epsilon H$ should resonate outside the diamagnetic envelope.

(36) de Ropp, J. S.; La Mar, G. N. In *Plant Peroxidases: Biochemistry and Physiology*; Welinder, K. G., Rasmussen, S. K., Penel, C., Greppin, H., Eds.; University of Geneva Press: Geneva, Switzerland, 1993; pp 43−55.

(37) Schonbaum, G. R. *J. Biol. Chem.* **1973**, *248*, 502−511. Schonbaum, G. R.; Lo, S. *J. Biol. Chem.* **1972**, *247*, 3353−3360.

(38) Veitch, N. C.; Williams, R. J. P. *Eur. J. Biochem.* **1990**, *189*, 351−362. Banci, L.; Bertini, I.; Bini, T.; Tien, M.; Turano, P. *Biochemistry* **1993**, *32*, 5825−5831.

(39) Sakurada, J.; Takahashi, S.; Hosoya, T. *J. Biol. Chem.* **1986**, *261*, 9657−9662.

(40) Ortiz de Montellano, P. R. *Acc. Chem. Res.* **1987**, *20*, 289−294.

(41) Uno, T.; Nishimura, Y.; Tsuboi, M. *J. Biol. Chem.* **1987**, *262*, 4549−4556.

(42) Neither LiP-CN nor MnP-CN exhibits[13] signals upfield of −2 ppm which can arise from the distal Arg.

(43) It is noted that, while the distal His $N_\delta H$, $N_\epsilon H$, and $C_\epsilon H$ dipolar shifts of CcP-CN, HRP-CN, LiP-CN, and MnP-CN are remarkably similar[10-13] (<5% variation in δ_{DSS}(obs)), the $C_\delta H$ δ_{DSS}(obs) is significantly further downfield (by ~50% or to 3−4 ppm) in MnP-CN/LiP-CN[13] compared to HRP-CN/CcP-CN.[10,11] Inspection of Figure 5C shows that the distal His $C_\delta H$ shift is the most sensitive to β, and correctly correlates with low-field bias of $\beta \rightarrow 0$.

Axial His Ring Shifts as Indicator of Imidazolate Character. The enhanced stability of oxidized states in heme peroxidase relative to myoglobin had been proposed to arise,[1,4,30,44] in part, from the coordinated His side chain exhibiting significant imidazolate character. The C*c*P crystal structure has shown[3,4] that the axial His ring NH serves as a hydrogen bond donor to the side chain of a conserved Asp, and mutation of this hydrogen bond acceptor destabilizes the oxidized states.[45] The strong upfield shift of a broad peak attributed[8c] to the axial His $C_\epsilon H$ in HRP-CN, C*c*P-CN, together with the influence of the deprotonation of the axial imidazole on the $C_\epsilon H$ shift in a model compound,[46] led to an early proposal[47] that the axial His $C_\epsilon H$ shift can serve as an indicator of the degree of imidazolate character. Implicit in this interpretation[47] was the assumption that primarily electronic (contact) influences had been monitored when HRP-CN and metMbCN were compared. However, upon developing a quantitative understanding of the origin of the hyperfine shift pattern for a coordinate His, first in metMbCN,[17] and now in HRP-CN, it is clear that variable dipolar shifts dominate the axial His ring resonance positions.

The present semiquantitative interpretation confirms large and highly variable dipolar contributions to the axial His ring shifts which likely dominate any influence from the expected small changes in imidazolate character.[48] The extreme sensitivity of the axial His ring hyperfine shifts to the major magnetic axis orientation is illustrated in the plots in Figure 7 which extend the simulation of δ_{dip}(calc) over a variable tilt (β) from the heme normal 5 to 25°, and tilt direction over the whole heme plane (α) 0 → 360°. It is noted that the δ_{dip}(calc) varies over 50 ppm for $C_\epsilon H$, $C_\delta H$ depending solely on the variation in the direction of a 15° tilt, and by 30 ppm by varying β by 20° for fixed α. It is also apparent that, by changing the direction of the tilt for $\alpha \sim 0$ to 180−270°, the relative spectral positions of the $C_\epsilon H$ and $C_\delta H$ are interchanged with respect to that of HRP-CN. Hence, it is concluded that, unless it can be confirmed that the magnetic axes or Fe-CN tilt are completely conserved, a correlation between the $C_\epsilon H$ hyperfine shift and imidazolate character in cyanide-inhibited heme peroxidases is likely fortuitous. A linear plot of axial His $C_\epsilon H$ shift versus peroxidase redox potential has been reported.[12b] Such a correlation may be informative if a correlation between redox potential and ligand tilt could be established.

Conclusions

The hyperfine shift pattern for nonheme protons in cyanide-inhibited horseradish and cytochrome *c* peroxidases can be interpreted in terms of the orientation of the paramagnetic susceptibility tensor. The dominant influences on the hyperfine shift pattern is the tilt from the normal of the major magnetic axis which can be correlated with tilt of the Fe-CN unit. The pattern of distinctive hyperfine shift pattern changes upon substrate binding to HRP, or with genetic origin of the peroxidase, is consistent with modulation of the Fe-CN tilt in a largely structurally conserved catalytic site. It is likely that the significant changes in the hyperfine shift pattern in cyanide-inhibited point mutant peroxidases can shed light on perturbations on the distal interactions with the coordinated ligand.

Acknowledgment. The authors are indebted to Drs. Jeffrey S. de Ropp, Jun Qin, Griselda Hernández, and Krishnakumar Rajarathnam for experimental assistance and valuable discussions and to Professor T. L. Poulos for providing the crystal coordinates for C*c*P-CN. This research was supported by a grant from the National Institutes of Health, GM 26226.

Supplementary Material Available: One table (chemical shifts for HRPCN and HRPCN:BHA) and three figures: (1S) portions of the 500-MHz WEFT-NOESY spectrum of HRP-CN with BNA, (2S) plot of observed dipolar shifts vs calculated dipolar shifts for C*c*P-CN, and (3S) chemical shift differences between HRP-CN and HRP-CN:BHA (4 pages). This material is contained in many libraries on microfiche, immediately follows this article in the microfilm version of the journal, and can be ordered from the ACS; see any current masthead page for ordering information.

JA942622O

(44) Nickolls, P. *Biochim. Biophys. Acta* **1962**, *60*, 217−228.
(45) Goodin, D. B.; McRee, D. E. *Biochemistry* **1993**, *32*, 3313−3324.
(46) Chacko, V. P.; La Mar, G. N. *J. Am. Chem. Soc.* **1982**, *104*, 7002−7007.
(47) La Mar, G. N.; de Ropp, J. S.; Chacko, V. P.; Satterlee, J. D.; Erman, J. E. *Biochim. Biophys. Acta* **1982**, *708*, 317−325.

(48) The interpretation of the axial His $C_\epsilon H$ shift in terms of imidazolate character also has other serious shortcoming. In the model compound,[46] complete deprotonation results in only a 10 ppm upfield bias for C_3H. The range of the axial His $C_\epsilon H$ shift in heme peroxidases[10−13] is over 20 ppm, and, when including metMbCN,[17] over 45 ppm. Therefore, it is clear the variable partial deprontonation of the axis His imidazole in proteins cannot account for the range of observed $C_\epsilon H$ shifts.